J. Innovative Eng. Nat. Sci., vol. 5, no. 1, pp. 225-242, 2025.
http://doi.org/10.61112/jiens.1564284

Journal of Innovative Engineering and Natural Science
(Yenilikçi Mühendislik ve Doğa Bilimleri Dergisi)
https://dergipark.org.tr/en/pub/jiens

Original Paper

Optimization of drilling parameters for minimizing delamination factor in biocomposites using multiple nonlinear neuro-regression and stochastic methods

Melih Savran[a,*], Mücahit Osman Türkan[a], Mustafa Öncül[a], Levent Aydin[a]

[a]*İzmir Katip Çelebi University, Department of Mechanical Engineering, İzmir-Türkiye.*

ARTICLE INFO

Article history:
Received
Received in revised form
Accepted

Available online

Keywords:
Biocomposites
Drilling
Delamination factor
Neuro-regression
Stochastic optimization

ABSTRACT

In this study, a novel design optimization strategy is proposed to enhance the drilling performance of HDPE/Washingtonia fiber biocomposites, considering operational parameters such as drill diameter (d), feed rate (f), and spindle speed (N). A detailed investigation utilizing multiple nonlinear neuro-regression analyses is conducted to predict the delamination factor (F_d), based on a dataset obtained from a literature study. 14 candidate mathematical functions are suggested for modelling, and their accuracy is assessed through $R^2_{training}$, $R^2_{testing}$, and $R^2_{validation}$ metrics, and boundedness check. The identified effective models are subsequently employed in optimization using modified version of four methods: Nelder-Mead (NM), Simulated Annealing (SA), Random Search (RS), and Differential Evaluation (DE). The optimum values for parameters f, N and d were determined to be 50 mm/min, 355 rev/min, and 5.00 mm respectively, resulting with the minimum F_d values as 1.11615.

I. INTRODUCTION

In recent years, there has been a growing interest in utilizing biofibers as reinforcement or filler materials in polymer matrix composites. This shift towards the incorporation of biofibers is largely driven by the increasing prevalence of environmental regulations and the growing consumer demand for eco-friendly materials. This has prompted manufacturers to seek sustainable alternatives to conventional materials [1]. The utilization of biocomposites, which harness local and renewable resources, offers considerable advantages in terms of sustainability. The development of such materials is informed by the principles of industrial ecology, eco-efficiency, and green chemistry, which shape future material innovations, products, and processes [2]. Furthermore, biocomposites have attracted attention due to their cost-effectiveness and biocompatibility in comparison to synthetic fiber-based composites [3]. However, the manufacturing processes for biocomposites frequently encounter difficulties associated with the natural fiber content, resulting in inconsistency and inadequate control. This highlights the necessity for comprehensive scientific investigation to enhance comprehension of the behavior, characteristics, and performance of these materials [4].

Drilling represents a fundamental machining process within the manufacturing industry. However, it is often subject to a number of issues, with delamination representing a particularly significant concern. Reducing delamination is crucial to improve the overall quality of the manufacturing process, as it significantly affects the

*Corresponding author. Tel.: +90-232-329-3535; e-mail: mlhsvrn@gmail.com

structural integrity, surface finish, working life and aesthetic quality of composite materials. Delamination compromises mechanical properties such as tensile strength and impact resistance, leading to potential failure under stress, which is critical in industries such as aerospace and automotive. It also affects the precision of machined surfaces, causing problems in assembly and alignment. In addition, delaminated components have a shorter lifetime due to crack propagation, increasing maintenance and replacement costs. Addressing delamination through rework can increase production costs, so optimizing drilling parameters such as spindle speed, feed rate and tool geometry, and using special techniques help prevent damage and improve production efficiency [5].

The optimization of delamination necessitates the careful selection of drilling parameters, including feed rate (f), drill diameter (d), and spindle speed (N) [6]. Figure 1 provides a schematic representation of the delamination process in composite materials.

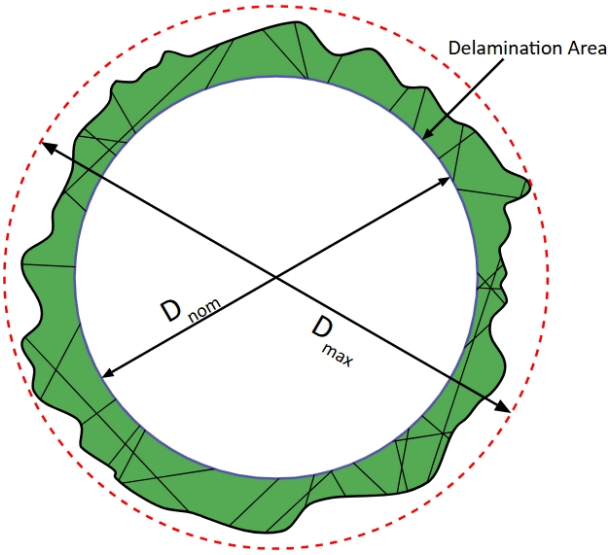

Figure 1. Schematic representations of delamination in a drilled hole

The delamination factor is defined as the ratio of the maximum diameter of the delaminated region surrounding the hole to the diameter of the hole itself. This is expressed by the following equation [7]:

$$F_d = \frac{D_{max}}{D_{nom}} \tag{1}$$

In a study conducted by Adda et al. [8], the optimization of delamination factors in the drilling of jute fiber-reinforced polymer biocomposites were investigated. In this study, experimental data was obtained by using Taguchi Method, and response surface methodology (RSM) and artificial neural networks (ANN) were applied to predict experimental results. The authors concluded that the optimal drilling conditions (feed rate = 50 mm/min, spindle speed = 1085.89 rev/min, and drill diameter = 5.00 mm) resulted in minimal delamination. In a recent study by AL-Oqla [7], the manufacturing process and delamination factor of cellulosic paper/epoxy composites, composed of 12, 25, and 50 paper layers, were examined. The results indicated that the optimal delamination factor

was achieved in the composite with 25 paper layers, using both 6 mm and 10 mm drill diameters at a spindle speed of 1500 rpm. This finding underscores the importance of selecting appropriate drilling parameters to enhance the structural performance of paper/epoxy composites. Belaadi et al. [4] employed an evaluation of the mechanical properties and the influence of drilling parameters on the delamination factor in jute fabric-reinforced epoxy matrix biocomposites. The study systematically varied spindle speed (355, 710, and 1400 rev/min), feed rate (50, 108, and 190 mm/min), and tool diameter (5, 7, and 10 mm) to assess their effects on the cutting process. Their findings revealed a significant relationship between these drilling parameters and the delamination factor, highlighting the critical role of precise parameter control in optimizing the structural integrity of drilled biocomposites. Design of experiments was developed by the application analysis of variance (ANOVA), and RSM and ANN methods were applied to predict the experimental results. The authors concluded that the ANN model showed better results as compared to RSM model. The Fd factor reached its optimal conditions with a feed rate of 51 mm/min, a spindle speed of 1160 rev/min, and a drilling diameter of 5 mm. In another work developed by Belaadi et al. [9], the drilling performance of HDPE/Washingtonia fiber biocomposites investigated. Full factorial method was used for design of experiments. Optimum drilling parameters were determined to be 50.13 mm/s feed rate, 806.00 rev/min spindle speed, and a drilling diameter of 5 mm. Tsao & Hocheng [10] examined the prediction and evaluation of the delamination factor when utilizing twist drills, candlestick drills, and saw drills. The aim of the research was to establish correlations between feed rate, spindle speed, and drill diameter, employing Taguchi's method and ANOVA. Ameur et al. [11] made an experimental investigation on the performances of thrust force, torque, exit delamination, and cylindricity error. They varied spindle speeds and feed rates, employing drills made of diverse materials. The study utilized RSM to establish correlations between cutting parameters and output responses across various drills. Optimal values for cutting parameters and the preferred tool material were determined through the desirability function approach.

The summary of the essential studies, their methodologies, and findings, providing a comprehensive overview of the current state of research on drilling performance and delamination in composite materials is given in Table 1.

Approaches such as RSM, ANN, and regression are easy to implement; however, they do not consider multiple objective criteria, and the ultimate optimal solution is highly responsive to the chosen dimensionality reduction techniques [12].

The present study proposes a new approach to address deficiencies in the design, modeling, and optimization of the drilling process. Multiple nonlinear neuro regression analysis includes the collaboration of ANN, regression analysis, and stochastic optimization methods to obtain suitable designs that satisfy the desired requirements. This method can offer a wide range of alternative mathematical models without limiting to specific polynomial forms or sigmoid, unit step, hyperbolic tangent activation functions. Additionally, model evaluation can incorporate both the R^2 value and the boundedness check criterion, offering a more comprehensive assessment. The boundedness check is essential for reliable mathematical model development. Since all engineering parameters are finite, realistic modeling in engineering systems requires boundedness. Thus, before optimization, verifying whether the models are bounded within the specified engineering parameter intervals is crucial. Unlike modeling approaches based on artificial neural networks (ANN), this method eliminates the need to fine-tune parameters such as the number of neurons and hidden layers, which are typically adjusted to optimize ANN-based models. With these

aspects, the proposed method substantially contributes to the modeling efforts related to the drilling process within literature.

Table 1. Summary of the studies on drilling performance and delamination in composites – methodologies and findings

Reference	Design Parameters	Research Focus	Modeling Methods	Key Findings
Adda et al. [8]	Spindle speed, feed rate, drill diameter	Optimization of delamination in jute fiber-reinforced polymer biocomposites	Taguchi Method, RSM, ANN	Optimal conditions: f = 50 mm/min, N = 1085.89 rev/min, d = 5.00 mm minimized delamination.
AL-Oqla [7]	Number of papers, spindle speed, drill diameter	Delamination in cellulosic paper/epoxy composites	Not specified	Optimal delamination factor achieved with 25 paper layers, using 6 mm and 10 mm drill diameters at 1500 rpm spindle speed.
Belaadi et al. [4]	Spindle speed, feed rate, drill diameter	Mechanical properties and delamination in jute fabric-reinforced epoxy biocomposites	RSM, ANN, ANOVA	Optimal conditions: f = 51 mm/min, N = 1160 rev/min, d = 5 mm. ANN model outperformed RSM.
Belaadi et al. [9]	Spindle speed, feed rate, drill diameter	Drilling performance in HDPE/Washingtonia fiber biocomposites	Full Factorial Method	Optimal parameters: f = 50.13 mm/s, N = 806.00 rev/min, d= 5 mm.
Tsao & Hocheng [10]	Spindle speed, feed rate, drill diameter	Prediction and evaluation of delamination factors with different drills	Taguchi's Method, ANOVA	Established correlations between f, N, and d for different drill types.
Ameur et al. [11]	Spindle speed, feed rate, tool material	Thrust force, torque, exit delamination, and cylindricity error	RSM	Optimal cutting parameters and tool material identified; correlations established using RSM.
Wang & Jia [12]	Spindle speed, feed rate	Comparison of modelling methods for delamination	RSM, ANN, Regression	Highlighted limitations of RSM, ANN, and regression in multi-objective optimization.
Başar et al. [13]	Multi-wall carbon nanotube content, cutting speed, feed rate	Modeling and optimization of thrust force in drilling glass fiber-reinforced polymer composites	Box-Behnken design, Desirability Function Analysis	Feed rate identified as the most influential factor affecting thrust force
Fedai et al. [14]	Multi-wall carbon nanotube weight percentage, cutting speed, feed rate	Optimization of thrust force and delamination factor in GFRP drilling	Grey Relational Analysis, ANOVA	Feed rate was confirmed as the most significant parameter affecting both thrust force and delamination factor
Der et al. [15]	Cutting power, cutting speed	Multi-criteria analysis for precise cutting of thermoplastics for thermal management systems	SWARA method, various multi-criteria decision-making methods	Optimal parameters for cutting polypropylene were found to be 90 W power and 15 mm/s cutting speed
Kaushik& Singh [16]	Drill point geometry, spindle speed, feed rate	Modeling and optimization of thrust force and delamination factor in drilling flax fiber-reinforced polymer composites	Teaching learning-based optimization, Genetic algorithm, Particle swarm	Drill point geometry was the most significant parameter affecting the thrust force, whereas spindle speed had the most negligible impact. Furthermore, the lowest and maximum thrust force and delamination factor were recorded for the U-shape drill bit.

The modeling and optimization methodology in paper is organized as follows: First, 14 candidate functional structures were proposed for modeling the drilling process using experimental data from the research by Belaadi et al. [9], and their accuracy is assessed based on R^2 training, R^2 testing, and R^2 validation values. Secondly, the boundedness of the candidate models has been checked. Lastly, the selected models utilized as objective function and delamination factor were optimized through four distinct methods: Nelder-Mead, Simulated Annealing, Random Search, and Differential Evaluation.

II. MATERIALS AND METHODS

2.1 Experimental Process

In the reference study [9], the researchers used Washingtonia filifera (WF) fibers obtained from desert palms grown locally in the Guelma region of Algeria. As matrix material, they used high-density polyethylene (HDPE) of 95% purity supplied by SABIC Petrochemicals. They produced the biocomposite material using two Thermotron-C.W. Brabender rollers to ensure complete blending and processing.

The researchers carried out the drilling tests using a high-performance MOMAC universal milling machine that supports feed rates from 4.6 to 1040 mm/rev and spindle speeds up to 1400 rpm. The dimensions of the biocomposite samples were 250 × 90 × 4 mm. They used high-speed steel drills with titanium nitride (HSS-TiN) coating and diameters of 5 mm, 7 mm and 10 mm. The feed rates of 50, 108 and 190 mm/min and spindle speeds of 355, 710 and 1400 rpm were adjusted for the delamination process. Damage assessment was carried out using the delamination factor (Fd) defined by the formula Fd = Dmax/D, where Dmax is the maximum diameter of the damaged area and D is the nominal diameter of the hole.

The present study carried out the mathematical modeling and optimization process using the experimental data set in the reference study [9].

2.2 Modeling

In the modelling phase, a hybrid method called Neuro-Regression which the synergy between regression analysis and ANN methodologies to enhance prediction accuracy. In this approach, the experimental data is first divided randomly into three datasets as 80%, 15%, and 5% of the given data; named as training dataset, testing dataset and validation dataset respectively.

First, 14 different mathematical models given in Table 2 alongside the training dataset were used for model fitting. Secondly, the $R^2_{training}$ values of these models were investigated to evaluate how good the models are at explaining the large portion of the variability in the training data. After the training step, these models were used to predict the results of the testing dataset to assess the performance of the models. $R^2_{testing}$ values were used in this part to see how good these models were at predicting a new, unseen dataset. Then, the $R^2_{validation}$ values, derived from the original and predicted values of the validation dataset, were investigated to see if there were any overfitting during the training phase, and for making fine tuning and adjustments on the candidate models [17, 18].

Table 2. Multiple regression model types include linear, quadratic, trigonometric, logarithmic, and their rational forms

Model Name	Nomenclature	Model
Multiple Linear	L	$a_0 + a_1x_1 + a_2x_2 + a_3x_3$
Multiple Linear Rational	LR	$(a_0 + a_1x_1 + a_2x_2 + a_3x_3)/(b_0 + b_1x_1 + b_2x_2 + b_3x_3)$
Second Order Multiple Nonlinear	SON	$a_0 + 2a_1x_1 + a_2x_1^2 + 2a_3x_2 + 2a_4x_1x_2 + a_5x_2^2 + 2a_6x_3 + 2a_7x_1x_3 + 2a_8x_2x_3 + a_9x_3^2$
Second Order Multiple Nonlinear Rational	SONR	$(a_0 + 2x_1a_1 + x_1^2a_2 + 2x_2a_3 + x_2^2a_5 + 2x_3a_6 + 2x_1x_3a_7 + 2x_2x_3a_8 + x_3^2a_9)/(b_0 + 2x_1b_1 + x_1^2b_2 + 2x_2b_3 + x_2^2b_5 + 2x_3b_6 + 2x_1x_3b_7 + 2x_2x_3b_8 + x_3^2b_9)$

Table 2 (Continued). Multiple regression model types include linear, quadratic, trigonometric, logarithmic, and their rational form

Third Order Multiple Nonlinear	TON	$a_0 + 3x_1a_1 + 3x_1^2a_2 + x_1^3a_3 + 3x_2a_4 + 6x_1x_2a_5 + 3x_1^2x_2a_6 + 3x_2^2a_7 + 3x_1x_2^2a_8 + x_2^3a_9 + 3x_3a_{10} + 6x_1x_3a_{11} + 3x_1^2x_3a_{12} + 6x_2x_3a_{13} + 6x_1x_2x_3a_{14} + 3x_2^2x_3a_{15} + 3x_3^2a_{16} + 3x_1x_3^2a_{17} + 3x_2x_3^2a_{18} + x_3^3a_{19}$
Fourth Order Multiple Nonlinear	FON	$a_0 + 4x_1a_1 + 6x_1^2a_2 + 4x_1^3a_3 + x_1^4a_4 + 4x_2a_5 + 12x_1x_2a_6 + 12x_1^2x_2a_7 + 4x_1^3x_2a_8 + 6x_2^2a_9 + 12x_1x_2^2a_{10} + 6x_1^2x_2^2a_{11} + 4x_2^3a_{12} + 4x_1x_2^3a_{13} + x_2^4a_{14} + 4x_3a_{15} + 12x_1x_3a_{16} + 12x_1^2x_3a_{17} + 4x_1^3x_3a_{18} + 12x_2x_3a_{19} + 24x_1x_2x_3a_{20} + 12x_1^2x_2x_3a_{21} + 12x_2^2x_3a_{22} + 12x_1x_2^2x_3a_{23} + 4x_2^3x_3a_{24} + 6x_3^2a_{25} + 12x_1x_3^2a_{26} + 6x_1^2x_3^2a_{27} + 12x_2x_3^2a_{28} + 12x_1x_2x_3^2a_{29} + 6x_2^2x_3^2a_{30} + 4x_3^3a_{31} + 4x_1x_3^3a_{32} + 4x_2x_3^3a_{33} + x_3^4a_{34}$
Hybrid Model	HM	$a_0 + 2x_1a_1 + x_1^2a_2 + 2x_2a_3 + 2x_1x_2a_4 + x_2^2a_5 + 2x_3a_6 + 2x_1x_3a_7 + 2x_2x_3a_8 + x_3^2a_9 + 2a_{10}\,log(x_1) + a_{11}\,log(x_1)^2 + 2a_{12}\,log(x_2) + 2a_{13}\,log(x_1)\,log(x_2) + a_{14}\,log(x_2)^2 + 2a_{15}\,log(x_3) + 2a_{16}\,log(x_1)\,log(x_3) + 2a_{17}\,log(x_2)\,log(x_3) + a_{18}\,log(x_3)^2$
Second Order Trigonometric Nonlinear	SOTN	$a_0 + 2a_1\,cos(x_1) + a_2\,cos(x_1)^2 + 2a_3\,cos(x_2) + 2a_4\,cos(x_1)\,cos(x_2) + a_5\,cos(x_2)^2 + 2a_6\,cos(x_3) + 2a_7\,cos(x_1)\,cos(x_3) + 2a_8\,cos(x_2)\,cos(x_3) + a_9\,cos(x_3)^2 + 2a_{10}\,sin(x_1) + 2a_{11}\,cos(x_1)\,sin(x_1) + 2a_{12}\,cos(x_2)\,sin(x_1) + 2a_{13}\,cos(x_3)\,sin(x_1) + a_{14}\,sin(x_1)^2 + 2a_{15}\,sin(x_2) + 2a_{16}\,cos(x_1)\,sin(x_2) + 2a_{17}\,cos(x_2)\,sin(x_2) + 2a_{18}\,cos(x_3)\,sin(x_2) + 2a_{19}\,sin(x_1)\,sin(x_2) + a_{20}\,sin(x_2)^2 + 2a_{21}\,sin(x_3) + 2a_{22}\,cos(x_1)\,sin(x_3) + 2a_{23}\,cos(x_2)\,sin(x_3) + 2a_{24}\,cos(x_3)\,sin(x_3) + 2a_{25}\,sin(x_1)\,sin(x_3) + 2a_{26}\,sin(x_2)\,sin(x_3) + a_{27}\,sin(x_3)^2$
Second Order Trigonometric Nonlinear Rational	SOTNR	$(a_0 + 2a_1\,cos(x_1) + a_2\,cos(x_1)^2 + 2a_3\,cos(x_2) + 2a_4\,cos(x_1)\,cos(x_2) + a_5\,cos(x_2)^2 + 2a_6\,cos(x_3) + 2a_7\,cos(x_1)\,cos(x_3) + 2a_8\,cos(x_2)\,cos(x_3) + a_9\,cos(x_3)^2 + 2a_{10}\,sin(x_1) + 2a_{11}\,cos(x_1)\,sin(x_1) + 2a_{12}\,cos(x_2)\,sin(x_1) + 2a_{13}\,cos(x_3)\,sin(x_1) + a_{14}\,sin(x_1)^2 + 2a_{15}\,sin(x_2) + 2a_{16}\,cos(x_1)\,sin(x_2) + 2a_{17}\,cos(x_2)\,sin(x_2) + 2a_{18}\,cos(x_3)\,sin(x_2) + 2a_{19}\,sin(x_1)\,sin(x_2) + a_{20}\,sin(x_2)^2 + 2a_{21}\,sin(x_3) + 2a_{22}\,cos(x_1)\,sin(x_3) + 2a_{23}\,cos(x_2)\,sin(x_3) + 2a_{24}\,cos(x_3)\,sin(x_3) + 2a_{25}\,sin(x_1)\,sin(x_3) + 2a_{26}\,sin(x_2)\,sin(x_3) + a_{27}\,sin(x_3)^2)/(b_0 + 2b_1\,cos(x_1) + b_2\,cos(x_1)^2 + 2b_3\,cos(x_2) + 2b_4\,cos(x_1)\,cos(x_2) + b_5\,cos(x_2)^2 + 2b_6\,cos(x_3) + 2b_7\,cos(x_1)\,cos(x_3) + 2b_8\,cos(x_2)\,cos(x_3) + b_9\,cos(x_3)^2 + 2b_{10}\,sin(x_1) + 2b_{11}\,cos(x_1)\,sin(x_1) + 2b_{12}\,cos(x_2)\,sin(x_1) + 2b_{13}\,cos(x_3)\,sin(x_1) + b_{14}\,sin(x_1)^2 + 2b_{15}\,sin(x_2) + 2b_{16}\,cos(x_1)\,sin(x_2) + 2b_{17}\,cos(x_2)\,sin(x_2) + 2b_{18}\,cos(x_3)\,sin(x_2) + 2b_{19}\,sin(x_1)\,sin(x_2) + b_{20}\,sin(x_2)^2 + 2b_{21}\,sin(x_3) + 2b_{22}\,cos(x_1)\,sin(x_3) + 2b_{23}\,cos(x_2)\,sin(x_3) + 2b_{24}\,cos(x_3)\,sin(x_3) + 2b_{25}\,sin(x_1)\,sin(x_3) + 2b_{26}\,sin(x_2)\,sin(x_3) + b_{27}\,sin(x_3)^2)$
Third Order Multiple Nonlinear Rational	TONR	$(a_0 + 3x_1a_1 + 3x_1^2a_2 + x_1^3a_3 + 3x_2a_4 + 6x_1x_2a_5 + 3x_1^2x_2a_6 + 3x_2^2a_7 + 3x_1x_2^2a_8 + x_2^3a_9 + 3x_3a_{10} + 6x_1x_3a_{11} + 3x_1^2x_3a_{12} + 6x_2x_3a_{13} + 6x_1x_2x_3a_{14} + 3x_2^2x_3a_{15} + 3x_3^2a_{16} + 3x_1x_3^2a_{17} + 3x_2x_3^2a_{18} + x_3^3a_{19})/(b_0 + 3x_1b_1 + 3x_1^2b_2 + x_1^3b_3 + 3x_2b_4 + 6x_1x_2b_5 + 3x_1^2x_2b_6 + 3x_2^2b_7 + 3x_1x_2^2b_8 + x_2^3b_9 + 3x_3b_{10} + 6x_1x_3b_{11} + 3x_1^2x_3b_{12} + 6x_2x_3b_{13} + 6x_1x_2x_3b_{14} + 3x_2^2x_3b_{15} + 3x_3^2b_{16} + 3x_1x_3^2b_{17} + 3x_2x_3^2b_{18} + x_3^3b_{19})$
First Order Logarithmic Multiple Nonlinear	FOLN	$a_0 + a_1\,log(x_1) + a_2\,log(x_2) + a_3\,log(x_3)$
First Order Logarithmic Multiple Nonlinear Rational	FOLNR	$(a_0 + a_1\,log(x_1) + a_2\,log(x_2) + a_3\,log(x_3))/(b_0 + b_1\,log(x_1) + b_2\,log(x_2) + b_3\,log(x_3))$
Second Order Logarithmic Multiple Nonlinear	SOLN	$a_0 + 2a_1\,log(x_1) + a_2\,log(x_1)^2 + 2a_3\,log(x_2) + 2a_4\,log(x_1)\,log(x_2) + a_5\,log(x_2)^2 + 2a_6\,log(x_3) + 2a_7\,log(x_1)\,log(x_3) + 2a_8\,log(x_2)\,log(x_3) + a_9\,log(x_3)^2$
Second Order Logarithmic Multiple Nonlinear Rational	SOLNR	$(a_0 + 2a_1\,log(x_1) + a_2\,log(x_1)^2 + 2a_3\,log(x_2) + 2a_4\,log(x_1)\,log(x_2) + a_5\,log(x_2)^2 + 2a_6\,log(x_3) + 2a_7\,log(x_1)\,log(x_3) + 2a_8\,log(x_2)\,log(x_3) + a_9\,log(x_3)^2)/(b_0 + 2b_1\,log(x_1) + b_2\,log(x_1)^2 + 2b_3\,log(x_2) + 2b_4\,log(x_1)\,log(x_2) + b_5\,log(x_2)^2 + 2b_6\,log(x_3) + 2b_7\,log(x_1)\,log(x_3) + 2b_8\,log(x_2)\,log(x_3) + b_9\,log(x_3)^2)$

Lastly, the boundedness check was made by examining the minimum and maximum values, derived from the differential evolution algorithm, of these candidate models in given intervals. This last process was done to see if the models were realistic or not.

2.3 Optimization

Structural optimization involves identifying the best design or a set of optimal designs by minimizing specified single or multiple objectives while ensuring that all constraints are met. Optimization methods can be categorized into traditional and non-traditional approaches. Traditional techniques, like constrained variation and Lagrange multipliers, are analytical and are only effective for continuous and differentiable functions. However, because composite design problems often involve discrete search spaces, these traditional methods are not suitable. Instead, stochastic optimization methods, such as genetic algorithms (GA) and simulated annealing (SA), are more appropriate for these scenarios [19]. In this study, the optimization problem is addressed using Modified Differential Evolution (MDE), Modified Nelder-Mead (MNM), Modified Simulated Annealing (MSA), and Modified Random Search (MRS) methods, all applied with their default settings.

The algorithms were implemented using Mathematica software. Mathematica's built-in functions, NMinimize and NMaximize, can be employed for both global and local optimization tasks. The optimization process can be performed by selecting the appropriate Nmimize and Nmaximize functions according to the desire to maximize or minimize the objective function. In addition, continuous and discrete constraints that will be included in the system can be directly added within these functions. In the present study, optimization problems were solved using the Nminimize solver.

2.3.1. Modified differential evolution algorithm

Differential Evolution (DE) is a population-based stochastic optimization algorithm introduced by Storn and Price in 1997. It is particularly well-suited for optimizing complex, nonlinear, and multi-modal objective functions, offering a robust alternative to traditional methods that may struggle in such scenarios. MDE operates by iteratively improving a population of candidate solutions through processes inspired by biological evolution, including mutation, crossover, and selection. In Mathematica, MDE is integrated into functions like NMinimize and NMaximize, providing a powerful tool for finding global optima in high-dimensional and complex search spaces. The algorithm's balance between exploration (searching broadly) and exploitation (refining promising areas) makes it highly effective for challenging optimization problems, offering users a reliable and efficient approach to optimize complex functions. [20].

2.3.2. Modified nelder-mead algorithm

The Nelder–Mead (NM) optimization algorithm is a straightforward direct search method that operates without the need for derivative information. It initiates the minimization process by employing a simplex. As the iteration progresses, the simplex may reach a flat configuration, signifying that the function's values are nearly identical across all vertices. The iterative steps of the Nelder-Mead algorithm involve ordering, centroid determination, and transformation [18]. While the Nelder–Mead algorithm is not designed as a global optimization method, it often works well in practice for problems with few local minima. Additionally, recent updates to the algorithm have extended its capabilities to handle constrained, discrete, and global optimization challenges [20].

2.3.3. Modified simulated annealing algorithm

Simulated Annealing (SA) is a probabilistic optimization algorithm inspired by the annealing process in metallurgy, where materials are heated and then gradually cooled to minimize energy states and reduce defects. It is particularly well-suited for global optimization in large and complex search spaces with multiple local optima. Mathematica integrates MSA into functions like NMinimize and NMaximize, allowing users to fine-tune several parameters to enhance performance.

Essential parameters influencing MSA include InitialPoints, which sets the starting location(s) in the search space. SearchPoints dictates the number of candidate solutions evaluated in each iteration. A higher number of search points ensures broader exploration but at a higher computational cost.

The RandomSeed parameter ensures the reproducibility of results by controlling the randomness in the algorithm, crucial for verifying and comparing different optimization runs. The Boltzmann Exponent determines how quickly the "temperature" decreases, affecting the likelihood of accepting suboptimal solutions during exploration. Level Iteration defines how many iterations the algorithm performs at each temperature level, controlling the depth of exploration. The effectiveness of MSA depends on carefully tuning these parameters. By adjusting these parameters, MSA can be optimized to solve a wide range of complex problems [21].

2.3.4. Modified random search algorithm

Random Search (RS) is a straightforward yet effective optimization algorithm, ideal for large, complex, or poorly defined search spaces. It differs from gradient-based methods in that it does not depend on derivative information but rather generates random candidate solutions within the search space and evaluates their performance based on the objective function. One of MRS's main strengths is its extensive exploration capability, reducing the likelihood of being trapped in local optima, a common limitation of more deterministic methods.

In Mathematica, RS is integrated into functions like NMinimize and NMaximize to search for global optima, particularly when the objective function is discontinuous, non-differentiable, or noisy. Despite its simplicity, MRS is widely applicable and can be combined with other techniques or used as a preliminary tool in complex optimization tasks.

Key parameters in MRS include InitialPoints, PenaltyFunction, SearchPoints, and PostProcess. The balance between the key parameters is critical to the success of MRS in identifying high-quality solutions [22]. The flowchart regarding mathematical modeling and optimization process is given in Figure 2 as follows.

2.4 Problem Definition

To determine design parameters effect of the drilling process on the delamination factor for HDPE/Washingtonia biocomposites, mathematical modelling and optimization studies were carried out using experimental data. The problem definition involved selecting a dataset, proposing mathematical models, and creating optimization scenarios to determine the most suitable design parameters and corresponding output for the drilling process. The dataset, taken from a reference study (Table 3), included the delamination factor output (F_d) and related design

parameters such as feed rate (f), spindle speed (N), and diameter (d) in the drilling process. Subsequently, 14 mathematical models were developed to describe the relationship between three design parameters and the output parameter based on the experimental data. The best model was chosen by evaluating R^2 training, R^2 testing, R^2 validation, and boundedness test results to represent the experimental data accurately. After selecting the appropriate model that provides boundedness criteria and gives the best R^2 values, three different optimization scenarios were defined. Modified version of stochastic optimization algorithms; MDE, NMM, MSA, MRS were utilized to solve the defined problems.

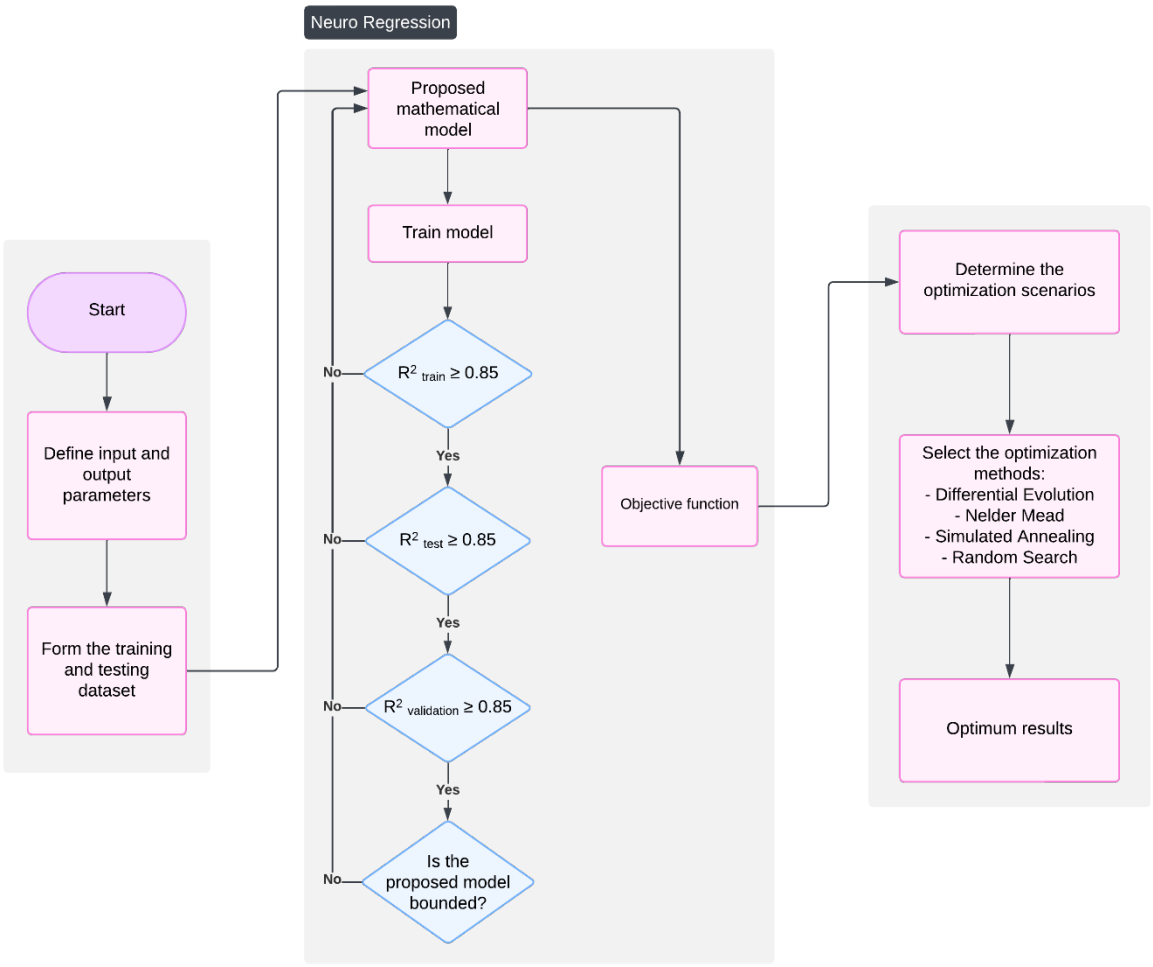

Figure 2. The flowchart regarding mathematical modeling and optimization process

2.5 Optimization Scenarios

The following scenarios were used to find the minimum delamination factor and corresponding optimum design variables. Furthermore, the effect of defined constraints in each scenario on the delamination factor was investigated.

Scenario 1. All the design variables are assumed to be real numbers within the continuous search space. The design variables range were set as follows: $50 \leq$ feed rate (f) ≤ 190, $355 \leq$ spindle speed (N) ≤ 1400, $5 \leq$ drill diameter (d) ≤ 10.

Scenario 2. The integer values of the design parameters are defined as a constraint in the system. The search space for design variables were set as follows: 50 ≤ feed rate (f) ≤ 190, 355 ≤ spindle speed (N) ≤ 1400, 5 ≤ drill diameter (d) ≤ 10.

Scenario 3. They were entered as a constraint in the system that the design parameters could only take certain specific values determined in the experimental set: feed rate (f) ∈{50, 108, 190}, spindle speed (N) ∈{355, 710, 1400}, drill diameter (d) ∈ {5, 7, 10}.

Table 3. Experimental data used in this research (Belaadi et al., 2022)[9]

f **(mm/min)**	N **(rev/min)**	d **(mm)**	Fd, EXP	Fd, RSM
50	355	5	1.1166	1.1176
108	355	5	1.1230	1.1223
190	355	5	1.1266	1.1267
50	710	5	1.1166	1.1167
108	710	5	1.1221	1.1212
190	710	5	1.1259	1.1253
50	1400	5	1.1176	1.1184
108	1400	5	1.1219	1.1224
190	1400	5	1.1261	1.1258
50	355	7	1.1222	1.1226
108	355	7	1.1261	1.1262
190	355	7	1.1274	1.1290
50	710	7	1.1230	1.1214
108	710	7	1.1250	1.1248
190	710	7	1.1273	1.1273
50	1400	7	1.1229	1.1225
108	1400	7	1.1261	1.1254
190	1400	7	1.1265	1.1273
50	355	10	1.1293	1.1289
108	355	10	1.1317	1.1309
190	355	10	1.1326	1.1314
50	710	10	1.1267	1.1273
108	710	10	1.1266	1.1290
190	710	10	1.1289	1.1292
50	1400	10	1.1278	1.1275
108	1400	10	1.1286	1.1288
190	1400	10	1.1289	1.1283

III. RESULTS AND DISCUSSIONS

This study established a mathematical relationship between design parameters (feed rate (x1), spindle speed (x2), drill diameter (x3), and output parameter (delamination factor (F_d)). The goal was to identify the values of these design parameters that minimize the delamination factor using the most effective model. The success of the mathematical models in meeting training, testing, validation, and boundedness control criteria is presented in Table 4. Upon reviewing Table 4, it becomes evident that all models performed remarkably well during the training phase, displaying high performance prediction levels close to 1 as per the R^2 criterion. Namely, all models successfully passed the training phase. However, during the testing phase, models including FON and SOTNR exhibited unacceptably low prediction performance levels. A similar assessment during the validation phase revealed that models such as FON, SOTN, and SOTNR displayed very low prediction performance. When considering the boundedness control criterion, it was determined that the maximum and minimum delamination factor values revealed by the SONR, SOTN, SOTNR and SOLNR models may not be unreasonable. As a result of these evaluations, it was seen that the FON SOTNR, SOTN, SONR, SOTN and SOLNR models did not meet the R^2 and boundedness check evaluation criteria. Among other models, models with an R^2 estimation performance of 0.85 and above in the training, testing and validation stages and which produced significant results according

to the boundedness check criterion were preferred as the objective function in the optimization process. LR and SOLN were the two models that met the mentioned conditions. While LR had 0.99, 0.86, 0.92 estimation performance in the training, testing and validation stages, respectively, these values were found to be 1, 0.88, 0.87 for the SOLN model.

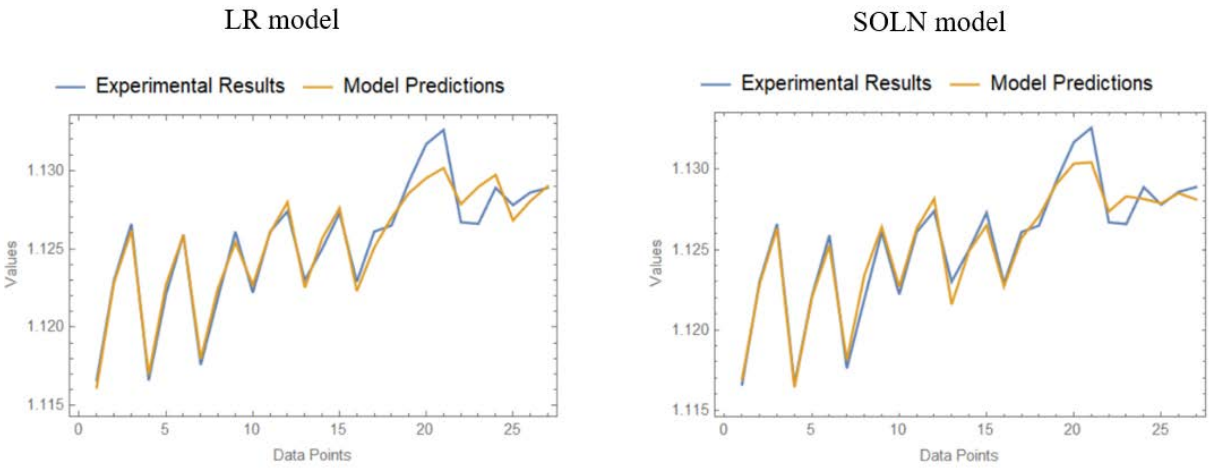

Figure 3. Comparison of LR and SOLN model prediction performance with experimental results

Figure 3 presents the experimental and predicted results for both the LR (Linear Rational) model and the SOLN (Second Order Logarithm Nonlinear) model. This figure allows a comparison between the observed and the predicted values of delamination factor for the two models. Both models produced predictions that were perfectly aligned with the experimental results up to the 18th data point. However, between the 18th and 25th data points, slight deviations between the predicted and experimental outcomes were observed. This range corresponds to the dataset that was allocated for testing and validation. Because the models attempt to predict data they have not previously encountered, these deviations are reasonable and expected.

Table 4. Proposed Mathematical models to explain inputs and output relation

Model	$R^2_{training}$	$R^2_{testing}$	$R^2_{validation}$	Minimum Fd	Maximum Fd
L	0.999998	0.644907	0.740797	1.11834	1.13315
LR*	0.999999	0.858051	0.923233	1.11615	1.13017
SON	0.999999	0.776201	0.965609	1.1166	1.13043
SONR	1	0.698208	0.855111	-1.1113E+11	174848
TON	1	0.784234	0.955925	1.11588	1.13187
FON	1	0.364962	0.464991	1.10921	1.13758
HM	1	0.77835	0.772345	1.11436	1.13161
SOTN	1	0.96258	0.58856	0.122134	1.2111
SOTNR	0.99596	-1951.82	-15810.6	-3934370	5735.77
TONR	0.999999	0.866178	0.778461	1.11651	1.13049
FOLN	0.999998	0.799344	0.611545	1.11793	1.13253
FOLNR	0.999999	0.878908	0.760117	1.11609	1.13037
SOLN*	1	0.876652	0.870804	1.11633	1.1305
SOLNR	1	0.772175	0.957495	-1587.15	4.08908

Full form of models was given in appendix.

Figure 4 graphically represents and compares the LR and SOLN model's behavior for design parameters d=5, 7, and 10. When the drill diameter is set to 5, an increase in spindle speed alone does not significantly affect the delamination factor in either model. However, an increase in feed rate is directly proportional to an increase in the

delamination factor. To achieve the lowest delamination factor, it is necessary to maintain both the feed rate and spindle speed parameters at their minimum levels.

LR model SOLN model

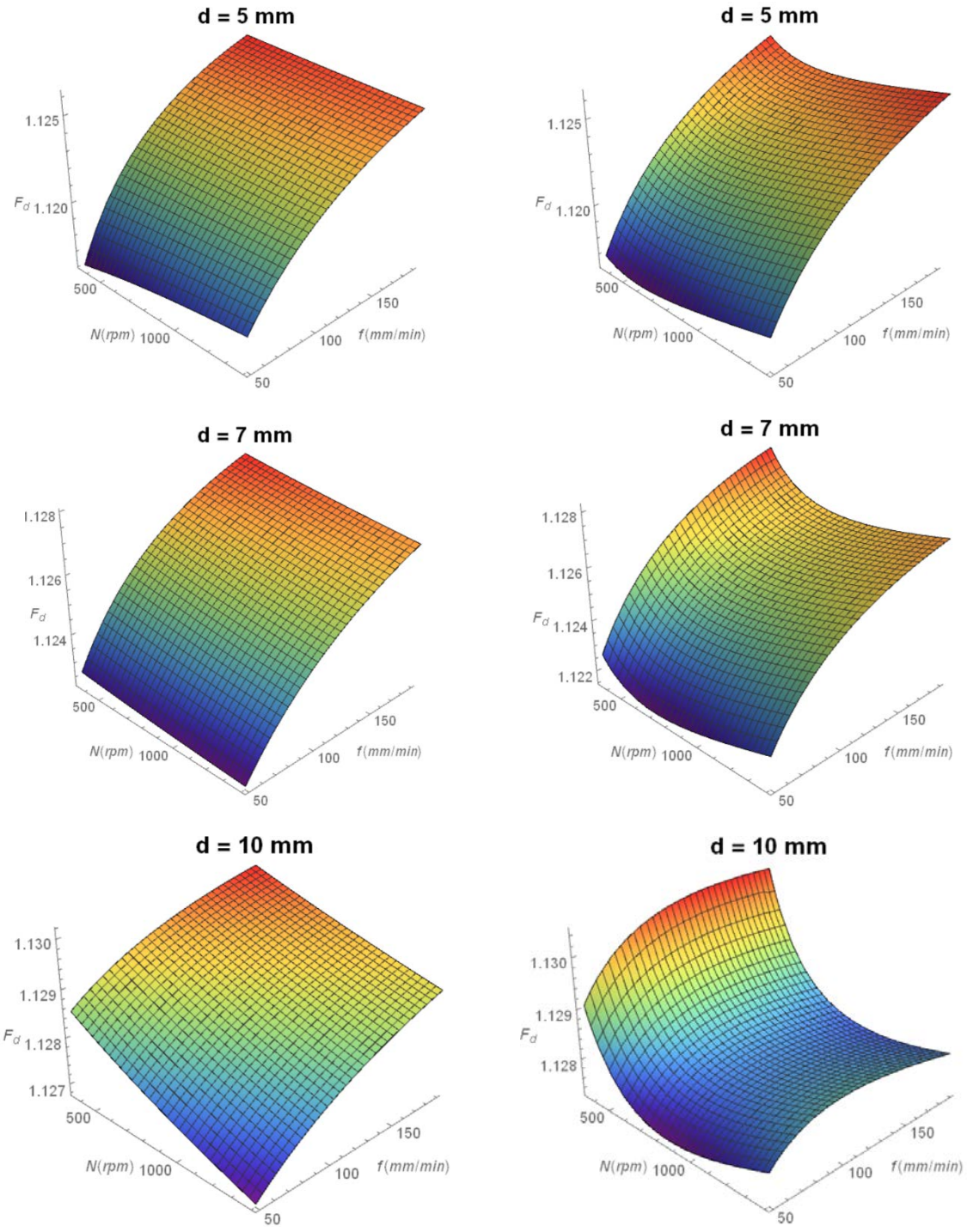

Figure 4. Comparison of LR and SOLN model regarding N, f, d design parameters and corresponding delamination factor

In contrast, when the drill diameter is set to 7, unlike the previous case (d=5), an increase in spindle speed in the LR model, without altering the feed rate, results in a slight decrease in the delamination factor. In the SOLN model, an initial increase in spindle speed leads to a reduction in the delamination factor, but as the spindle speed continues to rise, the delamination factor reverses its trend and begins to increase. The minimum delamination factor is observed when the feed rate is kept at its lowest, and the spindle speed is maintained at moderate levels.

Finally, when the drill diameter is adjusted to 10, the LR model predicts that the minimum delamination factor is achieved by increasing spindle speed while decreasing the feed rate. In the SOLN model, the lowest delamination factor is obtained by selecting moderate spindle speed and minimal feed rate. Notably, in the SOLN model, a decrease in spindle speed with a constant feed rate causes a sharp increase in the delamination factor, which stands out as a significant deviation compared to the other conditions.

The optimization results for the selected models using three different scenarios have been presented in Table 5. The drilling parameters f, N, and d are represented as x1, x2, and x3, respectively.

In the first scenario, all design parameters were set to be continuous within the search space. For the LR model, consensus was reached among the four algorithms on the values of the parameters f, N, and d, which were determined to be 50 mm/min, 355 rev/min, and 5.00 mm, respectively. Consequently, the minimum Fd value obtained was 1.11615. For the SOLN model, the optimal drilling parameters were identified as 50 mm/min, 586.4 rev/min, and 5.00 mm for f, N, and d, resulting in an Fd value of 1.11633.

In the second scenario, all design parameters were constrained to integer values within the defined search spaces. The MDE and MSA algorithms both identified an optimal F_d value of 1.11615 for the LR model, recommending drilling parameters of 50 mm/min, 355 rev/min, and 5.00 mm for f, N, and d, respectively. In contrast, the NM and RS algorithms appeared to be trapped in local minima, failing to reach the global optimum. Specifically, the NM algorithm identified the design parameters and drilling factor as f=51 mm/min, N=1400 rev/min, d=8 mm, with F_d=1.12406, while the RS algorithm determined f=96 mm/min, N=1101 rev/min, d=5 mm, and F_d=1.12187. For the SOLN model, the MDE algorithm suggested optimal drilling parameters of 50 mm/min, 586 rev/min, and 5.00 mm for f, N, and d, with an F_d value of 1.11633. The MSA algorithm provided a similar result, yielding an F_d value of 1.11634, with parameters f=50 mm/min, N=617 rev/min, and d=5 mm. As with the LR model, the MNM and MRS algorithms converged to local minima in the SOLN model and were unable to find the optimal solutions.

In the third scenario, the design variables were chosen based on the level values established during the creation of the experimental set. As a result of the optimization using the LR model, all four optimization algorithms produced the same results as the first scenario for the design parameters f, N, d, and drilling factor F_d. In this case, the design parameters were f = 50 mm/min, N = 355 rev/min, and d = 5 mm, resulting in an F_d value of 1.11615. When evaluating the optimization using the SOLN model, the design parameters were found to be f = 50 mm/min, N = 586.4 rev/min, and d = 5.00 mm, with the corresponding delamination factor F_d found to be 1.11642 using all algorithms.

Upon evaluating all the results in Table 5, it is evident that the optimal designs obtained using the LR model are slightly superior to those obtained using the SOLN model, as anticipated. This can be attributed to the LR model's better prediction performance compared to the SOLN model. While all algorithms produce similar results to each other in scenarios 1 and 3 for LR and SOLN models, different outcomes are observed in scenario 2. Notably, MDE emerges as the most successful algorithm in this scenario.

In the referenced study [9], response surface methodology (RSM) and artificial neural networks (ANN) were used as modeling approaches, with second-order polynomial and hyperbolic tangent models identified as the most successful. However, the RSM-based model lacked essential performance evaluation stages, such as testing and validation, thereby reducing its reliability. Furthermore, neither RSM nor ANN models performance were evaluated using a boundedness check criterion to ensure that the results are meaningful in an engineering context. In the present study, both the rational and first-order logarithmic nonlinear models underwent comprehensive testing and validation, and an additional boundedness check was applied to confirm the engineering relevance of the models' maximum and minimum outputs. As a result, when comparing the present modeling approach with traditional RSM, ANN, and regression methods used in similar studies, the findings suggest a higher reliability in the obtained results.

Table 5. Results of optimization for LR and SOLN models

Model	Scenario No.	Constraints	Optimization Algorithm	Minimum F_d	Suggested Design
LR	1	$50 \le x1 \le 190$, $355 \le x2 \le 1400$, $5 \le x3 \le 10$	DE	1.11615	x1 = 50, x2 = 355, x3 = 5
			NM	1.11615	x1 = 50, x2 = 355, x3 = 5
			SA	1.11615	x1 = 50, x2 = 355, x3 = 5
			RS	1.11615	x1 = 50, x2 = 355, x3 = 5
	2	$50 \le x1 \le 190$, $355 \le x2 \le 1400$, $5 \le x3 \le 10$, $\{x1, x2, x3\} \in$ Integers	DE	1.11615	x1 = 50, x2 = 355, x3 = 5
			NM	1.12406	x1 = 51, x2 = 1400, x3 = 8
			SA	1.11615	x1 = 50, x2 = 355, x3 = 5
			RS	1.12187	x1 = 96, x2 = 1101, x3 = 5
	3	$x1 \in \{50, 108, 190\}$, $x2 \in \{355, 710, 1400\}$, $x3 \in \{5, 7, 10\}$	DE	1.11615	x1 = 50, x2 = 355, x3 = 5
			NM	1.11615	x1 = 50, x2 = 355, x3 = 5
			SA	1.11615	x1 = 50, x2 = 355, x3 = 5
			RS	1.11615	x1 = 50, x2 = 355, x3 = 5
SOLN	1	$50 \le x1 \le 190$, $355 \le x2 \le 1400$, $5 \le x3 \le 10$	DE	1.11633	x1 = 50, x2 = 586.404, x3 = 5
			NM	1.11633	x1 = 50, x2 = 586.428, x3 = 5
			SA	1.11633	x1 = 50, x2 = 586.428, x3 = 5
			RS	1.11633	x1 = 50, x2 = 586.428, x3 = 5
	2	$50 \le x1 \le 190$, $355 \le x2 \le 1400$, $5 \le x3 \le 10$, $\{x1, x2, x3\} \in$ Integers	DE	1.11633	x1 = 50, x2 = 586, x3 = 5
			NM	1.12223	x1 = 82, x2 = 565, x3 = 6
			SA	1.11634	x1 = 50, x2 = 617, x3 = 5
			RS	1.12181	x1 = 50, x2 = 959, x3 = 7
	3	$x1 \in \{50, 108, 190\}$, $x2 \in \{355, 710, 1400\}$, $x3 \in \{5, 7, 10\}$	DE	1.11642	x1 = 50, x2 = 710, x3 = 5
			NM	1.11642	x1 = 50, x2 = 710, x3 = 5
			SA	1.11642	x1 = 50, x2 = 710, x3 = 5
			RS	1.11642	x1 = 50, x2 = 710, x3 = 5

In terms of optimization, a comparison between the present and reference studies reveals that the optimum values for feed rate and drill diameter were identified at the lowest tested levels, at 50 mm/min and 5 mm, respectively, in both studies. However, spindle speed showed variability across the algorithms applied in each study. A common finding in the literature indicates that a low feed rate and drill diameter, combined with a moderate to high spindle speed, are more favorable for minimizing the delamination factor in the drilling process [4, 8, 9].

V. CONCLUSIONS

The study focused on mathematical modelling and optimization of the drilling process parameters and delamination factor relationship of HDPE/Washingtonia fiber biocomposite materials. The research highlights the significance of optimizing process parameters such as drill diameter, feed rate, and spindle speed to improve drilling efficiency and reduce the common difficulty of delamination, which is an integral part of the structural

integrity of manufactured components. Traditional approaches with limited regression models and neglect of nonlinear effects are found to be inadequate for addressing the optimization challenges in biocomposite production. In this study, a new mathematical modelling method is proposed, which uses artificial neural networks and regression as a hybrid to model the drilling process of HDPE/Washingtonia material. With the neuro regression method, which eliminates the use of a limited number of models in modelling methods such as ANN and RSM, 14 different mathematical models were tested to express the drilling process mathematically. The best models among linear, rational, logarithmic, polynomial and trigonometric were selected based on assessment criteria such as R^2 and boundedness check. The minimum delamination factor was obtained using four stochastic optimization methods: MDE, NMM, MSA, and MRS. This enabled a comparison of the results and tested their reliability. The important results obtained in the present study are as follows:

i. Upon investigation of the 14 models, it was found that only the LR and SOLN models fulfilled the criteria for selection in the optimization process. These models exhibited appropriate R^2training, R^2testing, R^2validation values, as well as valid boundedness.
ii. When the LR and SOLN models were compared, the LR model gave smaller Fd value for Scenario 1 and Scenario 3.
iii. The optimum values of minimum delamination factor (F_d) and its corresponding design parameters were found as F_d= 1.11615, f=50 mm/min, N= 355 rev/min and d=5 mm, respectively.
iv. To the best of our knowledge, this study is the first to utilize the neuro-regression approach for model the delamination factor in biocomposite materials.

Future research could focus on examining the effects of critical design parameters, including material thickness, drilling geometry, and tool material, on the drilling process by applying Multiple Nonlinear Neuro Regression. Such a study holds significant potential to enhance understanding of these influences. Furthermore, the mathematical modeling of the drilling process for composites commonly derived from natural materials, such as flax, kenaf, ramie, and polylactic acid (PLA), could further demonstrate the Neuro Regression method advantages over traditional methods like artificial neural networks (ANN), regression techniques, and response surface methodology (RSM). This approach could offer deeper insights into material behavior, potentially establishing Neuro Regression as a robust alternative in composite material modeling.

REFERENCES

1. Lotfi, A., Li, H., & Dao, D. V. (2019). Effect of drilling parameters on delamination and hole quality in drilling flax fiber reinforced bio-composites. In Sustainable Design and Manufacturing 2018: Proceedings of the 5th International Conference on Sustainable Design and Manufacturing (KES-SDM-18) 5 (pp. 71-81)
2. Bharath KN, Basavarajappa S (2016) Applications of biocomposite materials based on natural fibers from renewable resources: a review. Sci Eng Compos Mater 23(2):123–133. https://doi.org/10.1515/secm-2014-0088
3. Nassar MMA, Alzebdeh KI, Alsafy MMM, Piya S (2023) Optimizing drilling parameters for minimizing delamination in polypropylene-date palm fiber bio-composite materials. J Braz Soc Mech Sci Eng 45(11). https://doi.org/10.1007/s40430-023-04528-9
4. Belaadi A, Boumaaza M, Amroune S, Bourchak M (2020) Mechanical characterization and optimization of delamination factor in drilling bidirectional jute fibre-reinforced polymer biocomposites. Int J Adv Manuf Technol 111(7):2073–2094. https://doi.org/10.1007/s00170-020-06217-6
5. Benyettou R, Amroune S, Slamani M, KILIÇ A (2023) Investigation of machinability of biocomposites: modeling and ANN optimization. Acad J Manuf Eng 21(1).

6. Geng D, Liu Y, Shao Z, Lu Z, Cai J, Li X, Zhang D (2019) Delamination formation, evaluation and suppression during drilling of composite laminates: a review. Compos Struct 216:168–186. https://doi.org/10.1016/j.compstruct.2019.02.099
7. AL-Oqla FM (2023) Manufacturing and delamination factor optimization of cellulosic paper/epoxy composites towards proper design for sustainability. Int J Interact Des Manuf 17(2):765–773. https://doi.org/10.1007/s12008-022-00980-4
8. Adda B, Belaadi A, Boumaaza M, Bourchak M (2021) Experimental investigation and optimization of delamination factors in the drilling of jute fiber–reinforced polymer biocomposites with multiple estimators. Int J Adv Manuf Technol 116(9):2885–2907. https://doi.org/10.1007/s00170-021-07628-9
9. Belaadi A, Boumaaza M, Alshahrani H, Bourchak M, Jawaid M (2022) Drilling performance prediction of HDPE/Washingtonia fiber biocomposite using RSM, ANN, and GA optimization. Int J Adv Manuf Technol 123(5–6):1543–1564. https://doi.org/10.1007/s00170-022-10248-6
10. Tsao CC, Hocheng H (2004) Taguchi analysis of delamination associated with various drill bits in drilling of composite material. Int J Mach Tools Manuf 44(10):1085–1090. https://doi.org/10.1016/j.ijmachtools.2004.02.019
11. Ameur MF, Habak M, Kenane M, Aouici H, Cheikh M (2017) Machinability analysis of dry drilling of carbon/epoxy composites: cases of exit delamination and cylindricity error. Int J Adv Manuf Technol 88(9–12):2557–2571. https://doi.org/10.1007/s00170-016-8967-8
12. Wang Q, Jia X (2021) Optimization of cutting parameters for improving exit delamination, surface roughness, and production rate in drilling of CFRP composites. Int J Adv Manuf Technol 117(11):3487–3502. https://doi.org/10.1007/s00170-021-07918-2
13. Başar G, Kırlı Akın H, Kahraman F (2020) Modelling and analysis of thrust force in drilling of nanocomposites using response surface methodology. Gazi Univ J Sci Part C Des Technol 8(2):293–305. https://doi.org/10.29109/gujsc.648188
14. Fedai Y, Basar G, Kirli Akin H (2022) Multi-response optimization in drilling of MWCNTs reinforced GFRP using grey relational analysis. Tech Vjesnik 29(3):742–751
15. Der O, Ordu M, Basar G (2024) Optimization of cutting parameters in manufacturing of polymeric materials for flexible two-phase thermal management systems. Mater Test 66(10):1700–1719
16. Kaushik D, Singh I (2024) Analysis of drilling behavior of flax/PP composites. Mater Manuf Process 39(8):1061–1073
17. Aydin L, Oterkus S, Artem HS (2020) Designing engineering structures using stochastic optimization methods. CRC Press, Boca Raton. https://doi.org/10.1201/9780429289576
18. Polatoğlu İ, Aydın L, Nevruz BÇ, Özer S (2020) A novel approach for the optimal design of a biosensor. Anal Lett 53(9):1428–1445. https://doi.org/10.1080/00032719.2019.1709075
19. Aydin L, Artem HS (2011) Comparison of stochastic search optimization algorithms for the laminated composites under mechanical and hygrothermal loadings. J Reinf Plast Compos 30(14):1197–1212. https://doi.org/10.1177/0731684411415138
20. Savran M, Aydin L, Ayaz A, Uslu T (2024) A new strategy for manufacturing, modeling, and optimization of 3D printed polylactide based on multiple nonlinear neuro regression analysis and stochastic optimization methods. Proc Inst Mech Eng Part E J Process Mech Eng. https://doi.org/10.1177/09544089241272909
21. Savran M, Aydin L (2023) Natural frequency and buckling optimization considering weight saving for hybrid graphite/epoxy-sitka spruce and graphite-flax/epoxy laminated composite plates using stochastic methods. Mech Adv Mater Struct 30(13):2637–2650. https://doi.org/10.1080/15376494.2022.2061656
22. Savran M, Sayi H, Aydin L (2020) Mathematica and optimization. In: Designing engineering structures using stochastic optimization methods, 1st Edition, CRC Press, Boca Raton, pp 24–43.

APPENDICES

APPENDIX A. Full form of the fitted models in Table 4.

Model Name	Nomenclature	Models
Multiple Linear	L	$Y = 1.11016 + 0.000042839x_1 - 1.13552 \times 10^{-6}x_2 + 0.00152511x_3$
Multiple Linear Rational	LR	$Y = (-519.377 + 12.8935x_1 + 0.497835x_2 + 132.416x_3)/(-440.664 + 11.3939x_1 + 0.443951x_2 + 115.43x_3)$
Second Order Multiple Nonlinear	SON	$Y = 1.09409 + 0.00018213x_1 - 2.51266 * 10^{(-7)}x_1^2 - 5.1393 * 10^{(-6)}x_2 - 4.27754 * 10^{(-9)}x_1x_2 + 4.26949 * 10^{(-9)}x_2^2 + 0.00445545x_3 - 0.0000114426x_1x_3 - 3.24234 * 10^{(-7)}x_2x_3 - 0.00010131x_3^2$
Second Order Multiple Nonlinear Rational	SONR	$Y = (-1.58142 * 10^8 + 911539x_1 - 7172.74x_1^2 - 8670.79x_2 + 4.48778x_2^2 + 5.59348 * 10^7x_3 + 23264.3x_1x_3 + 452.799x_2x_3 - 4.40876 * 10^6x_3^2)/(-1.38915 * 10^8 + 799876x_1 - 6353.56x_1^2 - 7732.93x_2 + 3.98358x_2^2 + 4.94452 * 10^7x_3 + 21365x_1x_3 + 404.802x_2x_3 - 3.90673 * 10^6x_3^2)$
Third Order Multiple Nonlinear	TON	$Y = 1.02447 + 0.000762679x_1 - 3.57252 * 10^{(-6)}x_1^2 + 8.54747 * 10^{(-9)}x_1^3 + 0.0000635067x_2 - 1.04997 * 10^{(-7)}x_1x_2 + 2.82805 * 10^{(-11)}x_1^2x_2 - 6.42632 * 10^{(-8)}x_2^2 + 4.53921 * 10^{(-11)}x_1x_2^2 + 1.91246 * 10^{(-11)}x_2^3 + 0.0205229x_3 - 0.0000683518x_1x_3 + 4.30151 * 10^{(-8)}x_1^2x_3 - 3.38983 * 10^{(-6)}x_2x_3 + 1.26738 * 10^{(-9)}x_1x_2x_3 + 2.46618 * 10^{(-9)}x_2^2x_3 - 0.00181595x_3^2 + 3.05343 * 10^{(-6)}x_1x_3^2 - 1.10434 * 10^{(-7)}x_2x_3^2 + 0.0000678489x_3^3$
Fourth Order Multiple Nonlinear	FON	$Y = 0.980295 + 0.000986753x_1 - 4.14279 \times 10^{-6}x_1^2 - 9.26588 \times 10^{-9}x_1^3 + 6.49449 \times 10^{-11}x_1^4 + 0.000067316x_2 - 8.16945 \times 10^{-8}x_1x_2 + 4.338 \times 10^{-11}x_1^2x_2 + 7.22689 \times 10^{-12}x_1^3x_2 - 7.83772 \times 10^{-8}x_2^2 - 9.01056 \times 10^{-11}x_1x_2^2 - 5.98033 \times 10^{-13}x_1^2x_2^2 - 7.90162 \times 10^{-12}x_2^3 + 3.37408 \times 10^{-14}x_1x_2^3 + 3.19808 \times 10^{-14}x_2^4 + 0.0278606x_3 - 8.91857 \times 10^{-6}x_1x_3 - 1.88944 \times 10^{-7}x_1^2x_3 + 7.90893 \times 10^{-10}x_1^3x_3 + 5.40496 \times 10^{-6}x_2x_3 + 9.39881 \times 10^{-9}x_1x_2x_3 - 2.14474 \times 10^{-10}x_1^2x_2x_3 - 3.44292 \times 10^{-9}x_2^2x_3 + 3.12031 \times 10^{-11}x_1x_2^2x_3 - 3.91792 \times 10^{-12}x_2^3x_3 - 0.00176114x_3^2 - 4.23002 \times 10^{-6}x_1x_3^2 + 1.08498 \times 10^{-8}x_1^2x_3^2 - 2.17128 \times 10^{-8}x_2x_3^2 - 1.08569 \times 10^{-9}x_1x_2x_3^2 + 8.08286 \times 10^{-10}x_2^2x_3^2 - 0.000152162x_3^3 + 3.13967 \times 10^{-7}x_1x_3^3 - 7.49399 \times 10^{-8}x_2x_3^3 + 0.0000163266x_3^4$
Hybrid Model	HM	$Y = (-61.9492 + 17.7266\,log(x_1) - 1.43955\,log(x_1)^2 + 1.28699\,log(x_2) - 0.964652\,log(x_1)\,log(x_2) + 0.106515\,log(x_2)^2 + 27.2315\,log(x_3) + 0.133602\,log(x_1)\,log(x_3) + 0.696741\,log(x_2)\,log(x_3) - 8.96799\,log(x_3)^2)/(-54.566 + 15.639\,log(x_1) - 1.2737\,log(x_1)^2 + 1.14463\,log(x_2) - 0.855412\,log(x_1)\,log(x_2) + 0.0938038\,log(x_2)^2 + 23.9843\,log(x_3) + 0.14251\,log(x_1)\,log(x_3) + 0.620307\,log(x_2)\,log(x_3) - 7.94651\,log(x_3)^2)$
Second Order Trigonometric Nonlinear	SOTN	$Y = 0.177446 + 0.18046\,cos(x_1) + 0.189259\,cos(x_1)^2 + 0.00176386\,cos(x_2) - 0.00287373\,cos(x_1)\,cos(x_2) + 0.236288\,cos(x_2)^2 + 0.0644773\,cos(x_3) - 0.00208998\,cos(x_1)\,cos(x_3) + 0.00121105\,cos(x_2)\,cos(x_3) + 0.268892\,cos(x_3)^2 + 0.152971\,sin(x_1) - 0.154314\,cos(x_1)\,sin(x_1) - 0.00234474\,cos(x_2)\,sin(x_1) + 0.00201114\,cos(x_3)\,sin(x_1) + 0.214092\,sin(x_1)^2 - 0.069922\,sin(x_2) - 0.00734882\,cos(x_1)\,sin(x_2) - 0.171164\,cos(x_2)\,sin(x_2) - 0.00092947\,cos(x_3)\,sin(x_2) - 0.00431512\,sin(x_1)\,sin(x_2) + 0.0766015\,sin(x_2)^2 - 0.0964769\,sin(x_3) + 0.00272514\,cos(x_1)\,sin(x_3) - 0.000070534\,cos(x_2)\,sin(x_3) + 0.173623\,cos(x_3)\,sin(x_3) - 0.00143825\,sin(x_1)\,sin(x_3) + 0.000916233\,sin(x_2)\,sin(x_3) + 0.279725\,sin(x_3)^2$
Second Order Trigonometric Nonlinear Rational	SOTNR	$Y = (1.02416 + 2.05291\,cos(x_1) + 1.01071\,cos(x_1)^2 + 2.02437\,cos(x_2) + 2.00063\,cos(x_1)\,cos(x_2) + 1.02648\,cos(x_2)^2 + 2.02522\,cos(x_3) + 1.99839\,cos(x_1)\,cos(x_3) + 2.0043\,cos(x_2)\,cos(x_3) + 1.01234\,cos(x_3)^2 + 2.04227\,sin(x_1) + 2.00181\,cos(x_1)\,sin(x_1) + 2.02175\,cos(x_2)\,sin(x_1) + 2.03232\,cos(x_3)\,sin(x_1) + 1.01345\,sin(x_1)^2 + 2.01017\,sin(x_2) + 2.02191\,cos(x_1)\,sin(x_2) + 2.00416\,cos(x_2)\,sin(x_2) + 1.95915\,cos(x_3)\,sin(x_2) +$

		$1.98707\,sin(x_1)\,sin(x_2) + 0.997679\,sin(x_2)^2 + 2.00457\,sin(x_3) + 2.00791\,cos(x_1)\,sin(x_3) + 1.9508\,cos(x_2)\,sin(x_3) + 2.03292\,cos(x_3)\,sin(x_3) + 1.99345\,sin(x_1)\,sin(x_3) + 1.97464\,sin(x_2)\,sin(x_3) + 1.01182\,sin(x_3)^2)/(0.982162 + 1.96055\,cos(x_1) + 0.991999\,cos(x_1)^2 + 1.97253\,cos(x_2) + 1.99801\,cos(x_1)\,cos(x_2) + 0.976149\,cos(x_2)^2 + 1.96414\,cos(x_3) + 1.99655\,cos(x_1)\,cos(x_3) + 1.99384\,cos(x_2)\,cos(x_3) + 0.9906\,cos(x_3)^2 + 1.9693\,sin(x_1) + 1.99877\,cos(x_1)\,sin(x_1) + 1.97905\,cos(x_2)\,sin(x_1) + 1.96071\,cos(x_3)\,sin(x_1) + 0.990163\,sin(x_1)^2 + 1.97365\,sin(x_2) + 1.96884\,cos(x_1)\,sin(x_2) + 1.98924\,cos(x_2)\,sin(x_2) + 2.04994\,cos(x_3)\,sin(x_2) + 2.00482\,sin(x_1)\,sin(x_2) + 1.00601\,sin(x_2)^2 + 1.97735\,sin(x_3) + 1.98231\,cos(x_1)\,sin(x_3) + 2.05264\,cos(x_2)\,sin(x_3) + 1.97151\,cos(x_3)\,sin(x_3) + 1.99898\,sin(x_1)\,sin(x_3) + 2.03598\,sin(x_2)\,sin(x_3) + 0.991562\,sin(x_3)^2)$
Third Order Multiple Nonlinear Rational	TONR	$Y = (1.00001 + 3.00308x_1 + 3.16091x_1^2 + 1.08627x_1^3 + 3.00681x_2 + 7.04699x_1x_2 + 3.77539x_1^2x_2 + 0.277339x_2^2 + 5.3307x_1x_2^2 - 0.0076471x_2^3 + 3.00036x_3 + 6.07393x_1x_3 + 3.2211x_1^2x_3 + 6.22103x_2x_3 + 6.99652x_1x_2x_3 + 3.6243x_2^2x_3 + 3.00257x_3^2 + 3.12472x_1x_3^2 + 3.34743x_2x_3^2 + 1.00205x_3^3)/ (0.999993 + 2.99656x_1 + 2.82165x_1^2 + 0.948349x_1^3 + 2.99249x_2 + 4.86762x_1x_2 + 3.371x_1^2x_2 + 6.09581x_2^2 + 4.72851x_1x_2^2 - 0.00782694x_2^3 + 2.99959x_3 + 5.91753x_1x_3 + 2.76832x_1^2x_3 + 5.75612x_2x_3 + 5.23857x_1x_2x_3 + 2.77635x_2^2x_3 + 2.99713x_3^2 + 2.86071x_1x_3^2 + 2.6186x_2x_3^2 + 0.99771x_3^3)$
First Order Logarithmic Multiple Nonlinear	FOLN	$Y = 1.09039 + 0.0044644\,log(x_1) - 0.000956056\,log(x_2) + 0.010563\,log(x_3)$
First Order Logarithmic Multiple Nonlinear Rational	FOLNR	$Y = (-184689. + 34427.7\,log(x_1) + 11678.9\,log(x_2) + 4916.17\,log(x_3))/(-162874. + 30430.4\,log(x_1) + 10417.7\,log(x_2) + 3967.76\,log(x_3))$
Second Order Logarithmic Multiple Nonlinear	SOLN	$Y = 1.04542 + 0.0349915\,log(x_1) - 0.00113135\,log(x_1)^2 - 0.0236313\,log(x_2) - 0.000607217\,log(x_1)\,log(x_2) + 0.0023575\,log(x_2)^2 + 0.0612321\,log(x_3) - 0.00870958\,log(x_1)\,log(x_3) - 0.00251446\,log(x_2)\,log(x_3) + 0.00131744\,log(x_3)^2$
Second Order Logarithmic Multiple Nonlinear Rational	SOLNR	$Y = (-61.9492 + 17.7266\,log(x_1) - 1.43955\,log(x_1)^2 + 1.28699\,log(x_2) - 0.964652\,log(x_1)\,log(x_2) + 0.106515\,log(x_2)^2 + 27.2315\,log(x_3) + 0.133602\,log(x_1)\,log(x_3) + 0.696741\,log(x_2)\,log(x_3) - 8.96799\,log(x_3)^2)/(-54.566 + 15.639\,log(x_1) - 1.2737\,log(x_1)^2 + 1.14463\,log(x_2) - 0.855412\,log(x_1)\,log(x_2) + 0.0938038\,log(x_2)^2 + 23.9843\,log(x_3) + 0.14251\,log(x_1)\,log(x_3) + 0.620307\,log(x_2)\,log(x_3) - 7.94651\,log(x_3)^2)$